

Inverse-Compton Emission from the Lobes of 3C353

Joanna Goodger, Martin Hardcastle and Judith Croston
University of Hertfordshire

Analysis of the radio synchrotron and X-ray inverse-Compton emission from radio-loud active galaxies allows us to determine their particle acceleration processes and electron energy spectra. Previous studies have provided new constraints on the energy budget and particle content of powerful radio galaxies and quasars; however, in most cases the sources are too faint in the X-ray to obtain spatial information in this way. We present archival and new, multi-frequency radio observations from the VLA and GMRT, and XMM observations of the bright FR II radio galaxy 3C353 which lies on the edge of the X-ray-luminous cluster Zw 1718.1-0108. The X-ray observations detect both the inverse-Compton emission from the radio galaxy lobes and thermal emission from the hot phase of the intercluster medium. We discuss the interaction between the cluster and the radio galaxy and describe the properties of the particle energy spectrum as a function of position in the lobe, as well as the properties of the merging cluster.

1. Introduction

3C353 is an FR II, radio-loud active galaxy associated with the cluster Zw 1718.1-0108 at $z=0.03$. The radio source resides in a giant elliptical galaxy on the edge of the cluster, which is bright in the X-ray with a luminous point source coinciding with the radio galaxy's core.

By studying radio galaxies like 3C353 in the radio and X-ray, we can determine the densities of the electrons emitting via synchrotron radiation in the radio and inverse-Compton emission in the X-ray. Studies of the radio emission alone cannot separate the effects of electron density and magnetic field strength. However, using X-ray data, the electron energy distribution can be measured directly. Understanding the influence of the electron densities of the synchrotron and inverse-Compton electron populations and the magnetic fields allows us to estimate the total energy in the radio source which can be transferred to the environment, and to investigate the distribution of internal energy within the source.

The radio data we use is a combination of VLA, multi-configuration data at 330 MHz, 1.4 GHz, 5 GHz and 8.4 GHz and GMRT data at 614 MHz. The VLA observations include new observations and archival data, all of which were calibrated using standard methods. Figure 1 shows an example of the image quality achieved. With these 5 frequencies of radio data and XMM X-ray data, the broad-spectrum electron energy distribution is well sampled. We also resolve the X-ray thermal emission from the cluster, shown in Figure 2, which extends beyond the field of view of XMM. Our radio data extends to lower frequencies than have been studied previously (Swain et al. 1998) whilst our X-ray data has greatly improved sensitivity and resolution over the existing ASCA observations (cf. Iwasawa et al. 2000).

2. Origin of the X-ray Emission

By considering the X-ray emission from regions encompassing the east and west lobes but excluding the hotspots and the core, we extracted spectra from the X-ray data set which we fitted with both thermal emission models and power-laws. The thermal fits for both lobes found unrealistic temperatures independent of the background region position, whereas the power-law model showed good fits, $\chi^2=45.9$ for 46 d.o.f for the east lobe and $\chi^2=23.7$ for 29 d.o.f for the west lobe. The photon indices were 2.0 ± 0.2 and 1.3 ± 0.3 respectively, consistent with an inverse-Compton model. This strongly suggests that the X-ray emission from the lobes is non-thermal in origin.

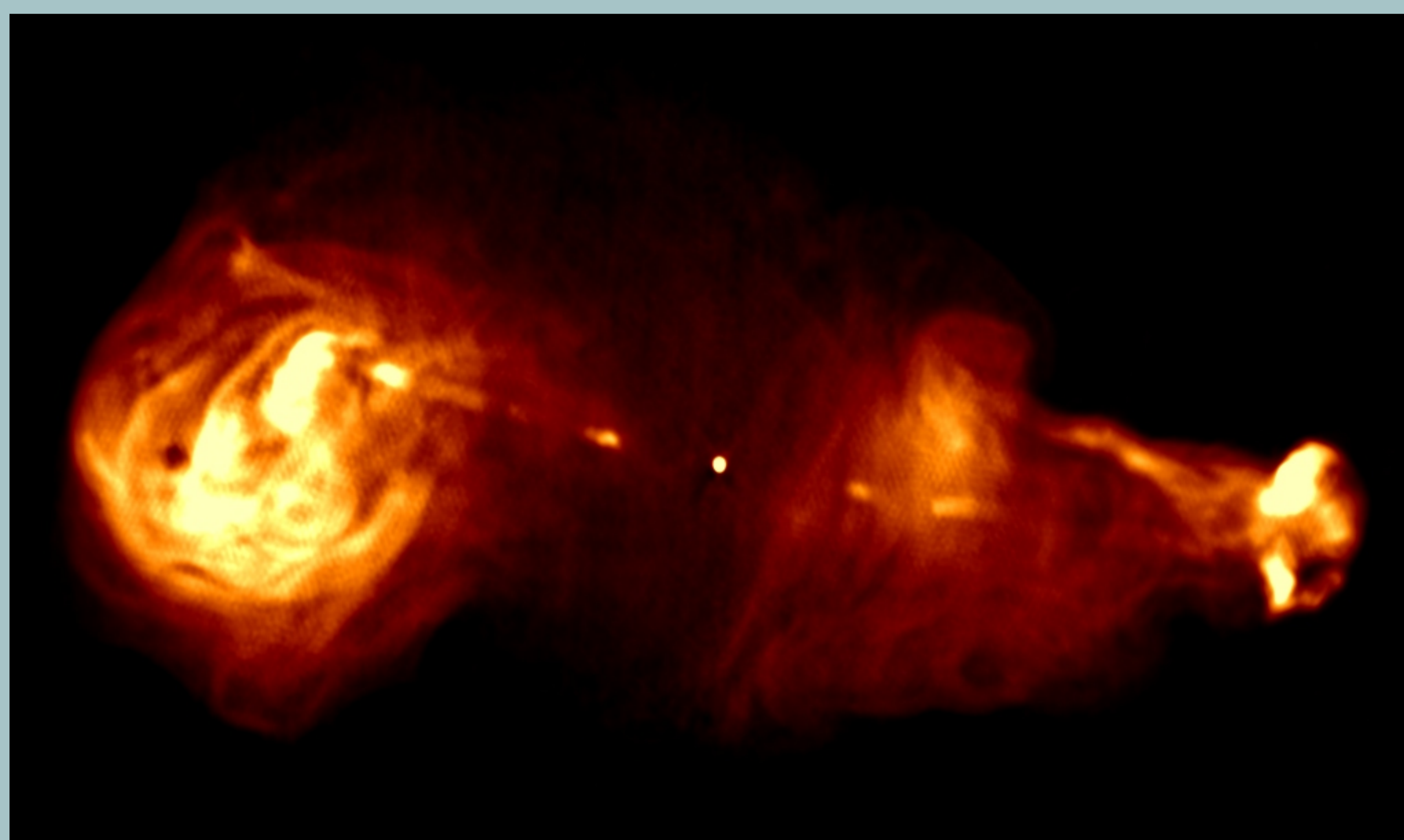


Figure 1: 1.4 GHz total intensity image of 3C353 at 1.8'' resolution

Using the multi-frequency radio data, we model the synchrotron emission and predict the form of the inverse-Compton emission at equipartition. The broad-band spectrum for the east lobe is shown in Figure 3. The equipartition inverse-Compton X-ray flux prediction for both lobes is less than the observed X-ray flux by a factor of ~ 2 . This difference lies within the range of this factor determined by Croston et al. (2005) using a sample of 33 FR II galaxies and quasars and indicates that the lobes of 3C353 are electron dominated. This factor would be reduced if the lobes are not in the plane of the sky.

3. Lobe Properties as a Function of Position

Constructing a spectral index map between the 1.4 GHz and 330 MHz images revealed a variation of ~ 0.1 across the east lobe. Within the radio luminous region of the east lobe, excluding the hotspots, the spectral index is roughly constant, ~ 0.66 , despite the filamentary structure seen in Figure 1. We note that the radio lobes do not appear to be entirely separate, and thus consider the region in between the radio luminous lobes, north and south of the core to be an inter-lobe region, which cannot be unambiguously associated with either lobe. This inter-lobe region has a relatively steep spectrum whereas the east hotspot exhibits a flatter spectrum.

We also observe a variation in the X-ray/radio ratio, with the steep inter-lobe region being a factor of 4 greater than the flat, hotspot regions. If the magnetic field strength and the number densities of both the inverse-Compton and synchrotron emitting electrons are constant across the lobe, the X-ray/radio ratio would be constant. As this is not what we observe, we examine the effect of varying either the magnetic field strength or the number densities as a function of position.

3.1 Electron Spectrum Variation

If we consider the magnetic field to be constant and apply an inverse-Compton model to the lobes, we find the emission at 330 MHz traces electrons with $\gamma=4500$ whilst the inverse-Compton emission traces electrons at $\gamma=1000$. As the critical frequency for synchrotron emission goes as γ^2 , we find that a variation in the X-ray/radio ratio of a factor of 4 requires a variation in the spectral index between 10 MHz and 330 MHz of ~ 0.46 . Even if the equipartition magnetic field strength is assumed so that the 330 MHz emission traces electrons of ~ 3000 , the observed spectral index variation requires a factor ~ 1.2 variation in the X-ray/radio ratio which is much lower than observed. We cannot therefore explain the observed variations with varying electron densities alone.

3.2 Magnetic Field Variation

If we assume constant electron densities for both the synchrotron and inverse-Compton emission electrons and also that the magnetic field strength does not vary along the line of sight, we find that the observed variation in the X-ray/radio ratio then requires a variation in the magnetic field of at most a factor 2.5. For a given frequency, the critical frequency goes as B^2 , so that the spectral indices observed at low frequencies, between 1.4 GHz and 330 MHz, for regions of high X-ray/radio ratio correspond to the spectral indices between 8.75 GHz and 825 MHz for low X-ray/radio ratio regions. We consider the spectral indices between 8.4 GHz and 1.4 GHz to limit the spectral indices of the low X-ray/radio ratio regions and find that they exceed the upper limit predicted by the observed X-ray/radio ratio.

We thus cannot rule out that a varying magnetic field alone could be responsible for the observed variations in the X-ray/radio ratio and the spectral indices; however, we conclude that a varying electron spectrum cannot account for these differences without the addition of a magnetic field variation. Similar conclusions were reached by Hardcastle and Croston (2005) in a study of Pictor A. Analysis of the detailed radio spectral properties will help us to see whether a model in which the electron spectrum is constant throughout the lobes is viable.

References

Croston, J.H., Hardcastle, M.J., Harris, D.E., Belsole, E., Birkinshaw, M. and Worrall, D.M., 2005, *ApJ* 626, 733
Hardcastle, M.J. and Croston, J.H., 2005, *MNRAS* 363, 649
Iwasawa, K., Etorri, S., Fabian, A.C., Edge, A.C. and Ebeling, H., 2000 *MNRAS* 313, 515
Swain, M.R., Bridle, A.H and Baum, S.A., 1998, *ApJ* 507, L29

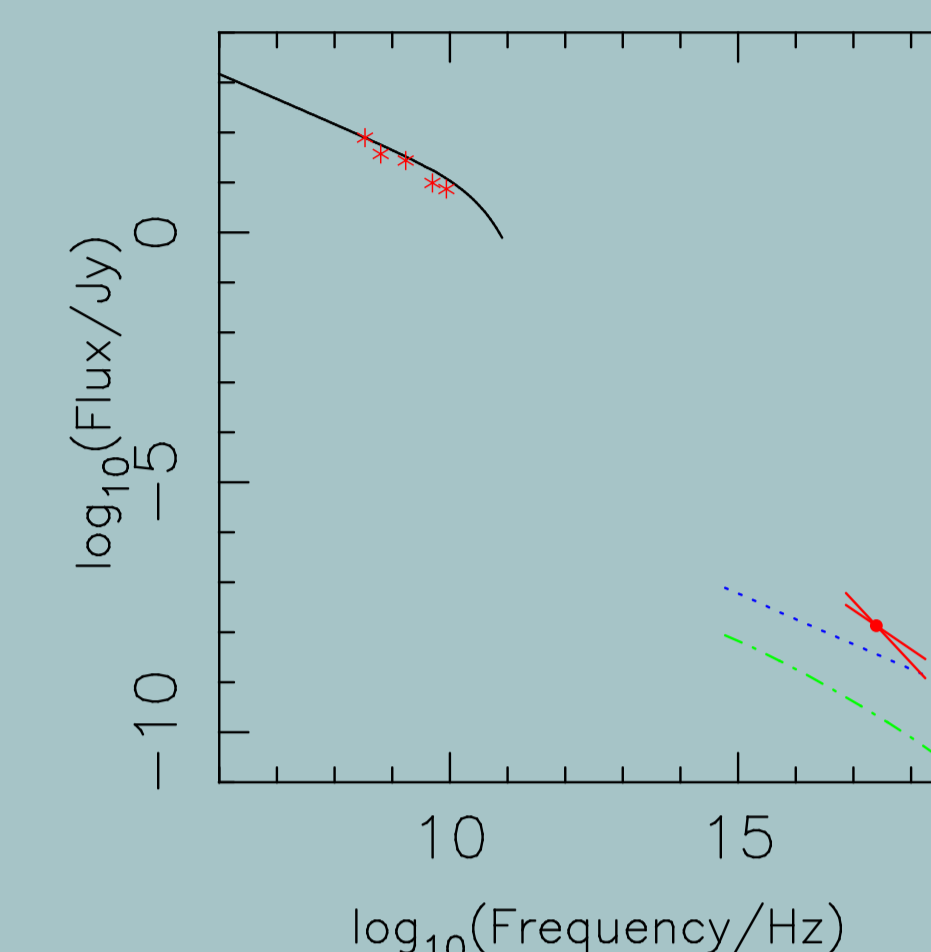


Figure 3: Broad-band spectra for the east lobe of 3C353. A synchrotron emission model (solid line) is fitted to the five frequency radio data (asterisks). The blue dotted line shows the inverse-Compton X-ray flux prediction for an equipartition magnetic field strength.

4. Characterisation of the Clusters

Also seen in the X-ray data set is the thermal emission from the cluster. Thermal fitting to the X-ray data sets for the north and south cluster regions has revealed a difference in mean temperature, with the northern cluster having $kT=3.0 \pm 0.1$ keV and the southern $kT=4.5 \pm 0.1$ keV. There appears to be no noticeable increase in temperature in between the two clusters, suggesting that the north and south clusters are not interacting violently.

We also note that there are no observed massive galaxies in the central region of the northern cluster as expected and as in seen in the southern cluster. There are three galaxies which were identified by Iwasawa et al. 1999; however, none of these occupy the northern cluster.

Using the surface brightness profiles, we will measure the densities of the clusters which, when combined with the temperature profiles, will allow us to determine the physical conditions and dynamics of the interaction between the cluster and the radio galaxy.

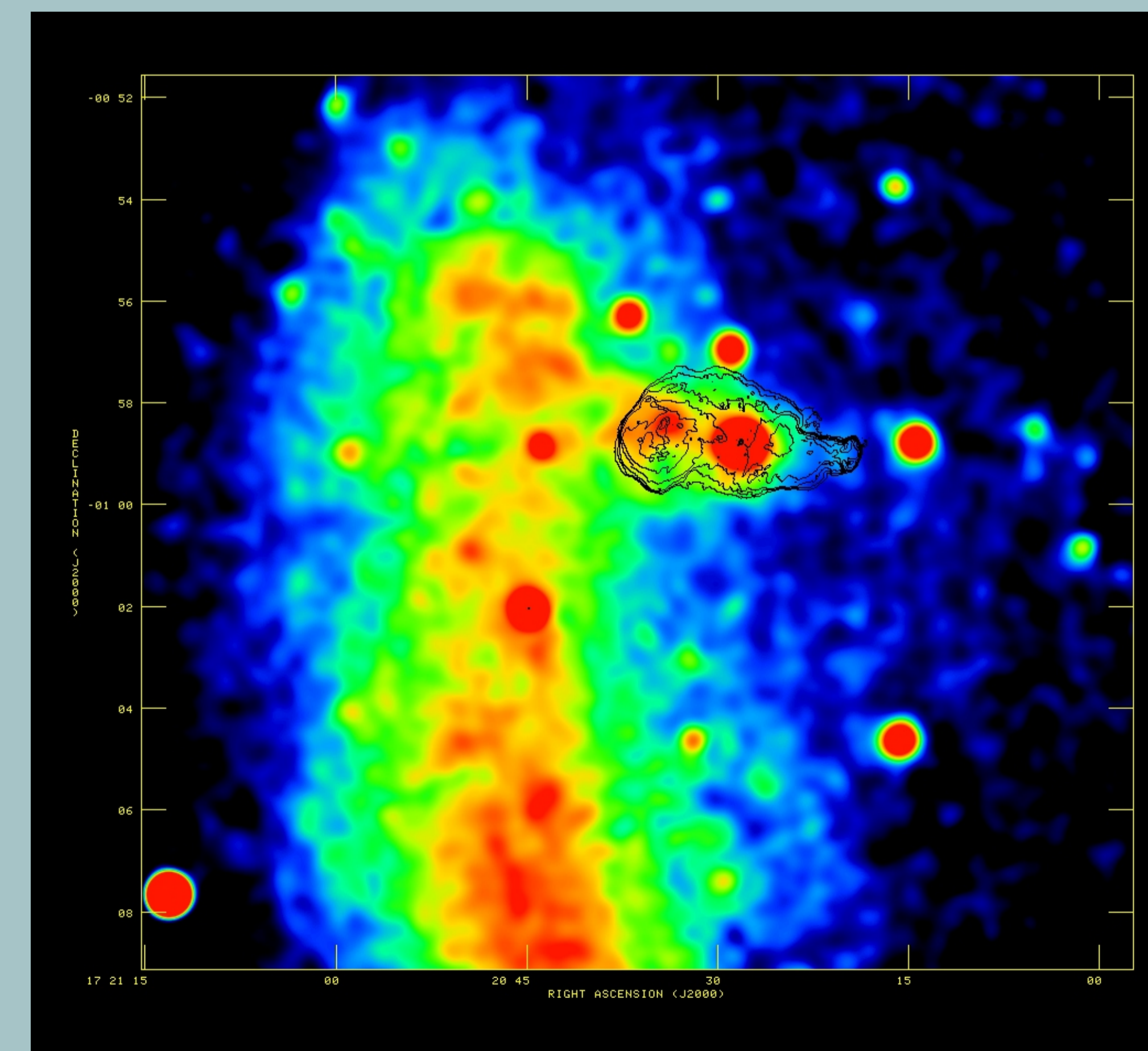


Figure 2: Radio contours of 3C353 with a Gaussian smoothed 0.3-7.0 keV XMM image (mos 1, mos 2 + pn) of the X-ray emission from the radio lobes and the cluster Zw 1718.1-0108